Shear Strength Assessment of RC Members: Influence of Shear Reinforcement and Yielding of the Flexural Reinforcement

Andrea Monserrat López[1*], Pedro Fco. Miguel Sosa [2]

1. PhD, Universitat Politècnica de València, Valencia, Spain
2. PhD, Dept. of Eng. Construction and Civil Eng. Projects, Universitat Politècnica de València, Valencia, Spain

[*]Corresponding author email: anmonlo6@upv.es

Abstract

An extensive experimental programme consisting of 15 shear tests on continuous reinforced concrete beams was carried out to assess the shear strength of beams with and without shear reinforcement. The influence of large flexural strains in the shear strength was analysed as the tests were designed to fail in shear after yielding of the flexural reinforcement.

The assessment of the shear strength was investigated based on the contribution of the various potential shear-transfer actions following the possibilities offered by Digital Image Correlation (DIC). In this field, several approaches accounting for the role of the various shear-transfer actions have recently been proposed, such as the Critical Shear Crack Theory or the Compression Chord Capacity Model, and significant advances on the analysis of the activation of these shear-transfer actions have been performed by the use of DIC.

In this work, detailed surface displacement measurements were performed by means of DIC, allowing to track the development and kinematics of the critical shear crack leading to failure. Based on this information, together with suitable constitutive models, the amount of shear transferred by each shear-transfer action was estimated at different load levels and at failure. The calculated shear strength of the specimens was obtained as the sum of the contribution of the various shear-transfer actions at failure and its comparison with the experimental results showed consistent agreement for the different cases.

Based on the results, different conclusions and implications about the contribution of the various shear-transfer actions at shear failure are presented. In general, the contribution of each shear-transfer action is strongly influenced by cracking patterns and by the location, shape and kinematics of the critical shear crack.

Keywords: *shear strength, reinforced concrete, shear reinforcement, digital image correlation, shear-transfer action.*

1. Introduction

1.1. Overview

Shear strength of reinforced concrete members has been extensively studied over the last decades. For members with shear reinforcement, equilibrium-based models (Schlaich, Schäfer and Jennewein 1987, Schlaich and Schäfer 1991) and stress fields (Muttoni, Schwartz and Thürlimann 1997) have proved to lead to safe approaches (ACI Committee 318 2019, EN 1992-1-1:2004). Also for members with shear reinforcement, the Modified Compression Field Theory (MCFT) (Vecchio and Collins 1986) has been widely extended and it is implemented in design code formulation (*fib* Bulletin 66 2012). On the other hand, for members without shear reinforcement, shear design has been traditionally based on empirical formulation calibrated from experimental results (ACI Committee 318 2019, EN 1992-1-1:2004). Nevertheless, although the extensive experimental work carried out to this aim, there is still no agreement about the role of the several shear-transfer actions at shear failure.

Some approaches, such as the Critical Shear Crack Theory (Muttoni and Fernández Ruiz 2008, Cavagnis et al. 2020) or the Compression Chord Capacity Model (Marí et al. 2015, Marí et al. 2016), account for the contribution of the various shear-transfer actions. These approaches explain the shear strength of members without shear reinforcement as the sum of the different actions (aggregate interlock, dowel action, residual tensile strength of concrete and the contribution of the compression chord), but the role attributed to each one is different. Despite this important difference, the shear strength predictions are comparable and fit reasonably well with experimental results.

Regarding the role of the various shear-transfer actions for members without shear reinforcement, the use of the Digital Image Correlation (DIC) has meant a great advance in recent years (Cavagnis, Fernández Ruiz and Muttoni 2018, Huber, Huber and Kollegger 2016). The accurate experimental measurements of the critical shear crack kinematics performed by DIC allow a better understanding of the contribution of the different actions and their governing parameters.

In this work, a detailed analysis of the various shear-transfer actions is presented for 15 continuous reinforced concrete beams with and without shear reinforcement tested by the authors (Monserrat López et al. 2020a, Monserrat López et al. 2020b). The information obtained from DIC measurements, together with suitable constitutive models, allowed obtaining the shear strength of each specimen as the sum of the various shear-transfer actions.

2. Experimental programme

2.1. Specimens

The experimental programme was presented in detail in Monserrat López et al. (2020a and 2020b). Regarding the continuous reinforced concrete beam tests, 15 beams (B1 to B15, Table 1) were tested with a test procedure divided into two different phases.

Specimens B1 to B9 were 9.00 m long and B10 to B15 were 7.00 m long (Fig. 1a). All of them had a rectangular cross section of 250 mm wide and 450 mm high (Fig. 1b). Specimens were divided into three series according to the shear reinforcement ratio (ρ_w): beams without shear reinforcement (R0), beams with ρ_w = 0.13% (R1) and beams with ρ_w = 0.20% (R2). Three sections were defined according to the flexural reinforcement ratio (ρ): beams with ρ = 1.63% (S1), beams with ρ = 2.29% (S2) and beams with ρ = 1.94% (S3) (Fig. 1b). Finally, specimens were tested under three different load and support points configurations according to the length of the span l_2. This length was 6.00 m (L6), 5.00 m (L5) and 4.00 m (L4) (Fig. 1b). Table 1 summarizes geometry and reinforcement of the specimens.

Table 1. Geometry and reinforcement of the specimens.

Specimen	Test	A_s	A'_s	ρ (%)	A_{sw}	ρ_w (%)	l_{tot} (m)	l_1 (m)	l_2 (m)	l_3 (m)	l_a (m)
B1	B1-R1-S1-L6	5ϕ20	7ϕ20	1.63	ϕ8/30	0.13	9.00	1.00	6.00	1.00	1.00
B2	B2-R1-S2-L6	7ϕ20	5ϕ20	2.29	ϕ8/30	0.13	9.00	1.00	6.00	1.00	1.00
B3	B3-R1-S3-L6	6ϕ20	6ϕ20	1.94	ϕ8/30	0.13	9.00	1.00	6.00	1.00	1.00
B4	B4-R1-S1-L5	5ϕ20	7ϕ20	1.63	ϕ8/30	0.13	9.00	1.62	5.00	1.00	1.00
B5	B5-R1-S2-L5	7ϕ20	5ϕ20	2.29	ϕ8/30	0.13	9.00	1.62	5.00	1.00	1.00
B6	B6-R1-S3-L5	6ϕ20	6ϕ20	1.94	ϕ8/30	0.13	9.00	1.62	5.00	1.00	1.00
B7	B7-R1-S1-L4	5ϕ20	7ϕ20	1.63	ϕ8/30	0.13	9.00	2.31	4.00	1.00	1.00
B8	B8-R1-S2-L4	7ϕ20	5ϕ20	2.29	ϕ8/30	0.13	9.00	2.31	4.00	1.00	1.00
B9	B9-R1-S3-L4	6ϕ20	6ϕ20	1.94	ϕ8/30	0.13	9.00	2.31	4.00	1.00	1.00
B10	B10-R0-S1-L4	5ϕ20	7ϕ20	1.63	-	-	7.00	1.00	4.00	1.00	0.70
B11	B11-R0-S2-L4	7ϕ20	5ϕ20	2.29	-	-	7.00	1.00	4.00	1.00	1.00
B12	B12-R0-S3-L4	6ϕ20	6ϕ20	1.94	-	-	7.00	1.00	4.00	1.00	0.89
B13	B13-R2-S1-L4	5ϕ20	7ϕ20	1.63	ϕ8/20	0.20	7.00	1.00	4.00	1.00	1.00
B14	B14-R2-S2-L4	7ϕ20	5ϕ20	2.29	ϕ8/20	0.20	7.00	1.00	4.00	1.00	1.00
B15	B15-R2-S3-L4	6ϕ20	6ϕ20	1.94	ϕ8/20	0.20	7.00	1.00	4.00	1.00	1.00

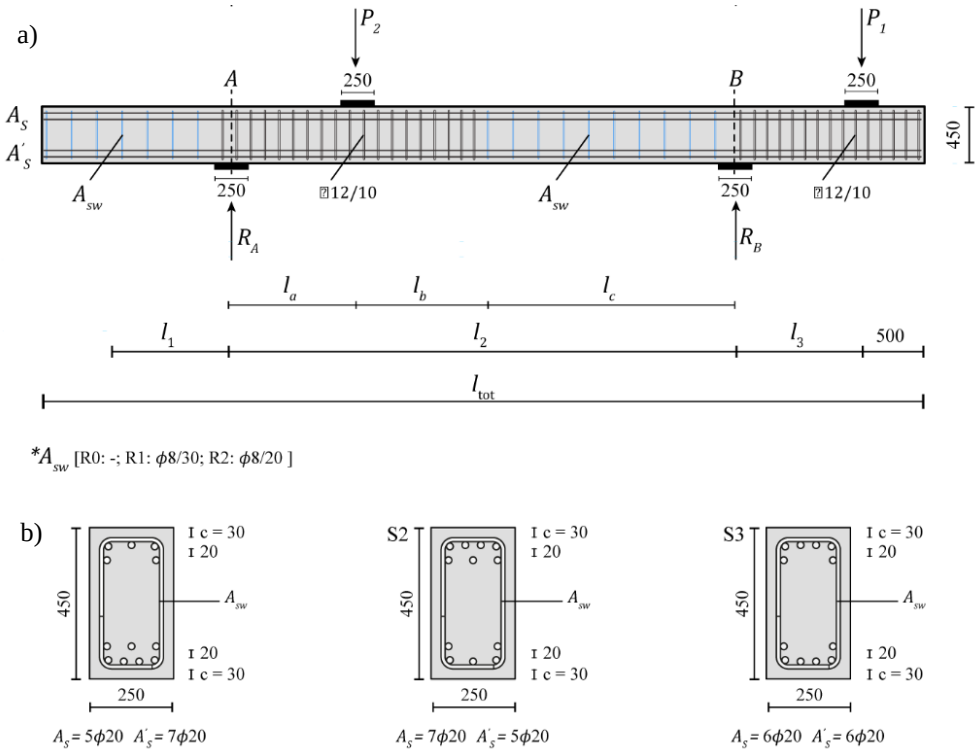

Figure 1. (a) Reinforcement, geometry and load arrangement of the tests; (b) flexural reinforcement of sections S1, S2 and S3 (dimensions in mm).

2.2. Test procedure

The 15 tests conducted on continuous reinforced concrete beams were developed in two phases (Fig. 1a). In the first phase, load P_1 was applied with displacement control, and load P_2 with load control according to P_1 to obtain no reaction at support A. This phase ended when the top flexural reinforcement at the support B section yielded. In the second phase, load P_2 was applied with displacement control until shear failure, and load P_1 was controlled to keep the slope at the support B constant and equal to the one reached at the end of the first phase. To maintain this slope, it was observed that a limited increase of load P_1 was required, which was responsible for additional rotations in the plastic hinge. It must be pointed out that the tests were designed to fail in shear after yielding of the flexural reinforcement.

2.3. Digital Image Correlation (DIC)

Apart from traditional instrumentation (strain gauges and displacement transducers), two-dimensional DIC was used to obtain accurate measurements of the cracking pattern on the regions where shear failure was expected. Photogrammetry was performed with Canon EOS 5D Mark II digital cameras (21.1 megapixels) with fixed-focus lens Canon EF 85 mm f/1.8 USM. The image acquisition rate during tests was variable, from images taken every two seconds at the beginning of the tests to a frequency up to 1 Hz at failure. The kinematics of the critical shear crack was obtained with the VIC2D software (Correlated Solutions 2009) from the displacement measurements. This kinematics was employed to calculate the various shear-transfer actions related to concrete contribution, such as aggregate interlock, residual tensile strength of concrete, dowel action and the contribution of the compression chord. The contribution of the shear reinforcement was obtained from an own software developed using NI-IMAQ driver and programming with LabVIEW. This software allowed measuring the critical shear crack opening along the vertical direction at the isolated location where the crack intercepts the different stirrups.

3. Analysis of the shear-transfer actions

The contribution of the various shear-transfer actions is obtained from the critical shear crack kinematics performed by DIC and by using constitutive models and calculation methodologies (Campana et al. 2013, Cavagnis, Fernández Ruiz and Muttoni 2018a, Cavagnis, Fernández Ruiz and Muttoni 2018b). The various shear-transfer actions refer to aggregate interlock (V_{agg}, Fig. 2), residual tensile strength of concrete (V_{res}, Fig. 2), dowel action ($V_{dow,t}$ in tension and $V_{dow,c}$ in compression, Fig. 2) and the contribution of the compression chord (V_{cc}, Fig. 2). The contribution of the transverse reinforcement (V_{sw}, Fig. 2) is considered for specimens with shear reinforcement (specimens B1 to B9 and B13 to B15, see Table 1).

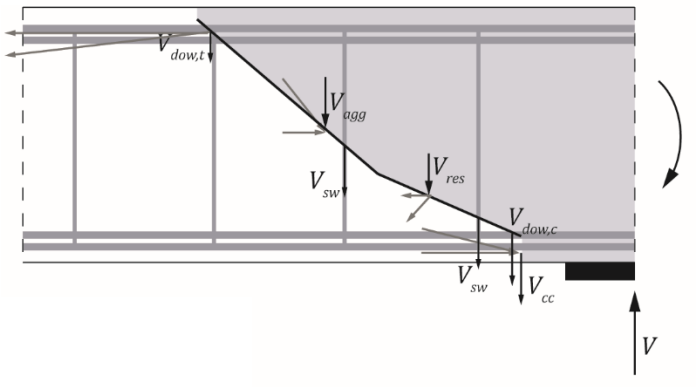

Figure 2. Shear-transfer actions: free body defined by the critical shear crack and internal forces (reinforced concrete members with shear reinforcement).

3.1. Aggregate interlock

The contribution of the aggregate interlock to the shear strength is obtained on the basis of the Two-Phase model developed by Walraven (1981) and the simplified kinematics proposed by Guidotti (2010). To this aim, the simplified formulas developed by Cavagnis, Fernández Ruiz and Muttoni (2018b) on these bases are used. The aggregate interlock interface stresses (normal stresses σ_{agg} and shear stresses τ_{agg}) are obtained from the crack opening w and the crack sliding δ as:

$$\sigma_{agg} = \sqrt{f_c} \cdot \frac{c_4 \cdot \bar{\delta}^{7/3}}{(c_2 \cdot \bar{w})^{3+c_2 \cdot \bar{\delta}}} \quad (1)$$

$$\tau_{agg} = \sqrt{f_c} \cdot \frac{c_3 \cdot \bar{\delta}^{4/3}}{(c_2 \cdot \bar{w})^{1.8+c_2 \cdot \bar{\delta}}} \quad (2)$$

where f_c is the compression strength of concrete; c_2 = 40, c_3 = 35 and c_4 = 400; $\bar{\delta} = \delta/d_{dg}$ and $\bar{w} = w/d_{dg}$ are the normalized crack sliding and crack opening respectively; d_{dg} is a parameter characterizing the roughness of the crack (Cavagnis, Fernández Ruiz and Muttoni 2018b).

Finally, the vertical component of the shear force transferred by the aggregate interlock across the critical shear crack is obtained by the integration of stresses according to:

$$V_{agg} = b \cdot \int_{\xi} \left(\tau_{agg} \sin\beta - \sigma_{agg} \cos\beta\right) d\xi \quad (3)$$

where b is the width of the section; ξ is the integration variable and β is the inclination of every segment of the polyline that approximates the shape of the critical shear crack.

3.2. Concrete residual tensile strength

The contribution of the concrete residual tensile strength to the shear strength is obtained from the expression suggested by Reinhardt (1985) that relates the residual tensile stresses (normal stresses σ_{res}) with the crack opening w as:

$$\sigma_{res} = f_{ct} \cdot \left(1 - \left(\frac{w}{w_{lim}}\right)^{c_1}\right) \quad (4)$$

where f_{ct} is the tensile strength of concrete; c_1 = 0.31 and $w_{lim} = G_F/f_{ct} \cdot (1 + c_1)/c_1$ is the limit crack width for stress transfer. The fracture energy G_F is calculated according to Model Code 2010 (*fib* Bulletin 66 2012).

Finally, the vertical component of the shear force transferred by the concrete residual tensile strength is obtained by the integration of stresses according to:

$$V_{res} = b \cdot \int_{\xi} \sigma_{res} \cos\beta \, d\xi \quad (5)$$

where b is the width of the section; ξ is the integration variable and β is the inclination of every segment of the polyline that approximates the shape of the critical shear crack.

3.3. Dowel action

The contribution of the dowelling action is obtained on the basis of the measured displacements of the concrete surface at the level of the flexural reinforcement (Cavagnis, Fenández Ruiz and Muttoni 2018a). The deflection of the flexural reinforcement in the horizontal distance influenced by the dowel action (l_{dow}, see Fig. 3) is approximated by a third-order polynomial ($v(x) = ax^3 + bx^2 + cx + d$) by considering the displacements of four points for each layer of flexural reinforcement (outer points PA1 and PB1 located at a distance $x_{dow} = \phi/2$ from points PA and PB, respectively, where ϕ refers to the diameter of the bar, see Fig. 3).

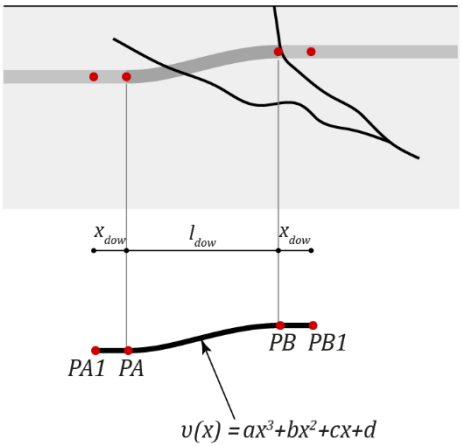

Figure 3. Dowel action of the flexural reinforcement: deflection of the flexural reinforcement in the horizontal length influenced by this phenomenon (Cavagnis, Fenández Ruiz and Muttoni 2018a).

The sectional curvature is obtained by differentiating two times the deflection $v(x)$. The strain of the central axis of the bar section is calculated from the horizontal displacement of the points PA and PB (see Fig. 3) and the length l_{dow}. Accounting for the curvature and the strain of the bar axis, the bending moment is calculated by considering a planar strain distribution and the shear force ($V_{dow,t}$ and $V_{dow,c}$) is calculated as the derivative of the bending moment.

3.4. Contribution of stirrups

The contribution of the shear reinforcement to the shear strength is the sum of the shear forces carried by each stirrup intercepted by the critical shear crack. In general, two stirrups are intercepted by this crack in the series R1 and three in the case of the series R2. The stirrups intercepted by the propagation of the horizontal branch of the critical shear crack are not considered in the contribution of the shear reinforcement, but in the contribution of the dowelling forces (Campana et al. 2013, Huber, Huber and Kollegger 2016).

The procedure proposed and validated by Campana et al. (2013) is followed to obtain the contribution of the shear reinforcement for the tested specimens. At the location where the critical shear crack (i) intercepts each stirrup, its vertical opening is obtained from the measured displacements of the concrete surface at two points (j and k) vertically aligned with the stirrup (see Fig. 4a). The rigid-plastic bond behaviour stablished by Sigrist (1995) is considered (see Fig. 4b). On this basis, and by considering a bilinear stress-strain relationship with strain hardening for the steel (see Fig. 4c) and the measured crack widths, the stresses and strains in a stirrup are determined (see Fig. 4d). As the procedure neglects the concrete strains, the crack opening is obtained by integrating the strains distribution of a stirrup along the tributary length ($l_{cont,i}$) of the crack.

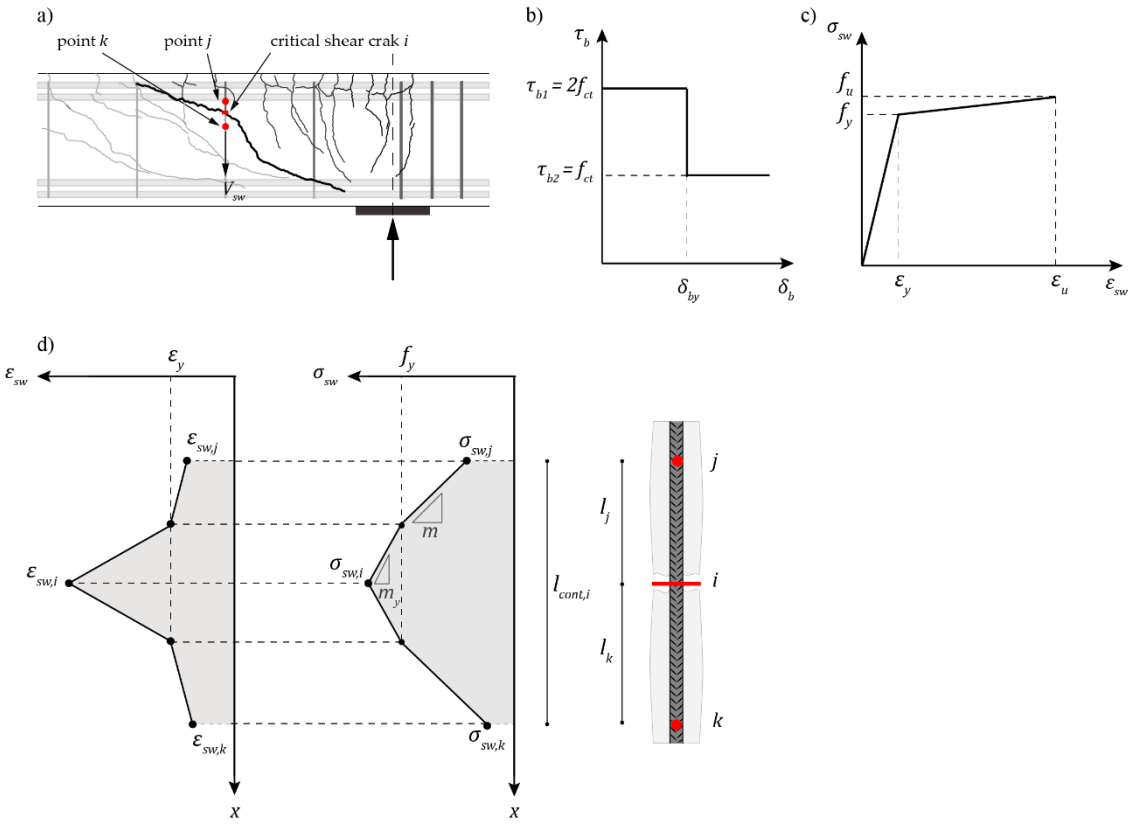

Figure 4. Shear reinforcement contribution: (a) obtaining the vertical crack opening of the critical shear crack by DIC; (b) the considered rigid-plastic bond behaviour; (c) the considered bilinear hardening stress-strain relationship of steel; (d) transmission of stresses and strains in a stirrup (Campana et al. 2013).

Finally, the shear force carried by each stirrup (V_{sw}) activated by the critical shear crack is calculated from the tensile stress (σ_{sw}) according to:

$$V_{sw} = 2 \cdot \sigma_{sw} \cdot \frac{\phi^2 \cdot \pi}{4} \tag{6}$$

where ϕ is the diameter of the bar (stirrup with two branches) and σ_{sw} is the tensile stress of the stirrup, which is calculated following the procedure of Campana et al. (2013).

3.5. Contribution of the compression chord

The contribution of the compression chord to the shear strength is obtained from the approach developed by Cavagnis, Fernández Ruiz and Muttoni (2018b). The resultant of the forces of the compression zone is composed of a horizontal force (N_{cc}) and a vertical one (V_{cc}), which define the inclination of the compression chord (α_{cc}) according to the simplified stress field presented in Figure 5. It is assumed that at the section AB the stress distribution increases linearly from zero at the tip of the crack to the extreme compression fibre ($c_n = 1/3\ h_T$, where h_T is the thickness of the compression zone below the

tip of the critical shear crack, see Fig. 5). It is also assumed that at the section CD the stress distribution is almost constant, corresponding to a stress block of thickness c_{m2} with a compressive stress equal to σ_c (see Fig. 5). According to these considerations, the contribution of the compression chord is:

$$V_{cc} = N_{cc} \cdot \tan \alpha_{cc} = \sigma_c \cdot c_{m2} \cdot b \cdot \frac{1/3 \cdot h_T - c_{m2}/2}{r_T} \quad (7)$$

where b is the width of the section and r_T is the horizontal distance between the vertical sections AB and CD (see Fig. 5).

From equation (7), the values r_T and h_T are obtained by DIC measurements, the value of the compressive stress σ_c can be assumed equal to the compressive strength of concrete f_c and the parameter c_{m2} can be assumed to be equal to c_m (effective depth of the stress block at the edge of the support plate).

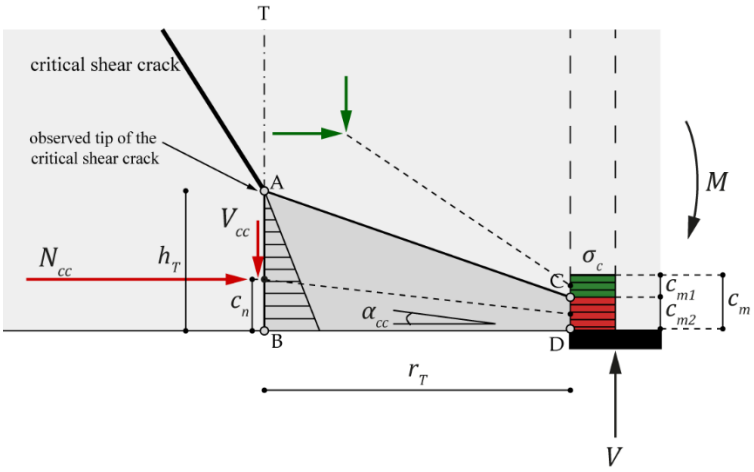

Figure 5. Hypothesis of the stress field used to determine the contribution of the compression chord (adapted from Cavagnis, Fenández Ruiz and Muttonin 2018b).

4. Analysis of the shear-transfer actions for the tested specimens

4.1. Main results at shear failure

Based on the procedures described previously, the amount of shear carried by each action is obtained at several load steps. In Table 2, the contribution of the various shear-transfer actions to the shear strength at failure is presented for the tested specimens (results of the test B11-R0-S2-L4 are not presented as a consequence of an inaccurate reading of crack kinematics). In this table, the percentage of the shear carried by each action over the experimental shear strength $V_{R,test}$ (values in brackets), the sum of the estimated contributions ($V_{R,calc}$) and the comparison between the experimental shear strength and the calculated shear strength ($V_{R,test}/V_{R,calc}$) are included.

The results show good agreement between the shear strength obtained from the estimated contribution of the various shear-transfer actions and the experimental shear strength. The average of the measured-to-calculated strength is 1.09, with a Coefficient of Variation equal to 15.4%. For members with shear reinforcement (specimens B1 to B9 and B13 to B15), the average of the measured-to-calculated strength is 1.06, with a Coefficient of Variation equal to 14.6%.

Table 2. Contribution of the various shear-transfer actions to the shear strength at failure.

Test	V_{agg} (kN)	V_{res} (kN)	$V_{dow,t}$ (kN)	$V_{dow,c}$ (kN)	V_{cc} (kN)	V_s (kN)	$V_{R,calc}$ (kN)	$V_{R,test}$ (kN)	$V_{R,test}/V_{R,cald}$
B1-R1-S1-L6	0.9 (0.7)	0.0	0.2 (0.1)	29.0 (20.8)	0.0	121.2 (86.9)	151.3	139.4	0.92
B2-R1-S2-L6	21.8 (15.3)	0.0	0.1 (0.0)	0.0	22.9 (16.1)	111.7 (78.4)	156.4	142.4	0.91
B3-R1-S3-L6	5.5 (3.8)	0.0	21.6 (14.9)	25.0 (17.2)	0.0	124.0 (85.4)	176.1	145.1	0.82
B4-R1-S1-L5	0.4 (0.3)	0.0	3.8 (2.7)	29.7 (20.8)	0.0	127.0 (88.8)	160.9	143.1	0.89
B5-R1-S2-L5	2.6 (1.4)	0.0	16.5 (8.7)	32.4 (17.2)	0.0	119.7 (63.4)	171.2	188.7	1.10
B6-R1-S3-L5	13.7 (7.2)	0.0	0.3 (0.1)	21.7 (11.3)	0.0	116.4 (61.0)	151.9	190.8	1.26
B7-R1-S1-L4	43.0 (19.9)	10.6 (4.9)	2.3 (1.1)	8.7 (4.0)	0.0	116.8 (54.0)	181.4	216.3	1.19
B8-R1-S2-L4	35.7 (17.8)	8.0 (4.0)	9.4 (4.7)	11.8 (5.9)	0.0	96.7 (48.1)	161.6	200.9	1.24
B9-R1-S3-L4	14.0 (7.3)	0.0	8.6 (4.4)	14.8 (7.7)	0.0	116.8 (60.7)	154.1	192.3	1.25
B10-R0-S1-L4	45.6 (55.4)	6.7 (8.1)	2.5 (3.0)	0.4 (0.4)	4.4 (5.3)	0.0	59.5	82.4	1.38
B12-R0-S3-L4	63.5 (72.5)	1.8 (2.1)	0.1 (0.1)	2.2 (2.5)	4.5 (5.2)	0.0	72.1	87.6	1.21
B13-R0-S3-L4	13.0 (6.0)	0.0	8.3 (3.8)	24.8 (11.4)	0.0	175.3 (80.6)	221.4	217.6	0.98
B14-R2-S1-L4	8.5 (3.8)	0.0	17.4 (7.8)	0.0	0.0	172.0 (77.3)	197.9	222.5	1.12
B15-R2-S2-L4	4.7 (2.4)	0.0	1.2 (0.6)	3.9 (1.9)	0.0	174.5 (87.6)	184.3	199.1	1.08

4.2. Evolution of the shear-transfer actions contribution

Figure 6 shows the kinematics of the critical shear crack and the contribution of the various shear-transfer actions at selected load steps for the tested specimen B7 (test B7-R1-SI-L4). It is a specimen with stirrups that fails in shear after the development of one plastic hinge at support B section (see Fig. 1a). In this case, the contribution of the shear reinforcement is governing (54% of $V_{R,test}$). The contribution of the aggregate interlock is also important (19.9% of $V_{R,test}$), as the critical shear crack develops steep segments that allows enhancing engagement of interlock stresses. The residual strength shows a limited contribution (4.9% of $V_{R,test}$), as well as the dowel action (1.1% of $V_{R,test}$ in tension and 4.0% of $V_{R,test}$ in compression). Finally, as a consequence of the location of the critical shear crack tip, there is no contribution of the inclined compression chord.

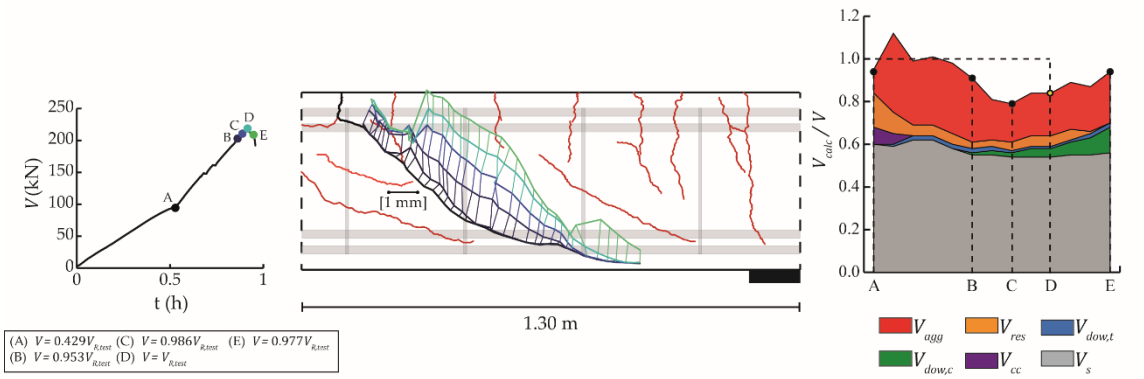

Figure 6. Evolution of the kinematics of the critical shear crack and the contribution of the various shear-transfer actions at selected load steps for the test B7-R1-S1-L4 (shear failure occurs at the step D and the step A corresponds to the development of the plastic hinge).

5. Conclusions

In this work, a detailed analysis of the contribution of the various shear-transfer actions to the shear strength of continuous reinforced concrete beams with and without shear reinforcement, based on DIC measurements, is presented. The main conclusions are the following:

1. At failure, the sum of the contribution of the various shear-transfer actions adequately explains the experimental values of shear strength obtained for the tested specimens.
2. The location, shape and kinematics of the critical shear crack govern the amount of shear carried by each shear-transfer action. The location of the tip of the critical shear crack determines the thickness of the compression zone, which highly influences the contribution of the inclined compression chord.
3. For the specimens with stirrups, the contribution of the shear reinforcement is dominant. The crack pattern determines the number of stirrups accounted for contributing to shear strength and the shear force transferred by each of them. The relative contribution of this action to the shear strength is comparable regardless of the shear reinforcement ratio of specimens.
4. The contribution of the aggregate interlock varies largely among the tested specimens. This shear-transfer action is governing for the specimens without stirrups. For the specimens with shear reinforcement, aggregate interlock is more significant in the steeper part of the critical shear crack. In these specimens, the yielding of the flexural reinforcement allows the critical shear crack to develop steeper, which results in the activation of a lower number of stirrups and a higher engagement of aggregate interlock in the steeper part of the critical shear crack.
5. The contribution of the dowel action significantly reduces with the yielding of the flexural reinforcement and low openings of the critical shear crack, but it can be significant for specimens with stirrups. In general, an increase of critical shear crack openings implies a reduction of the force transferred by aggregate interlocking, but an increase of the shear transferred by the dowel action.

Acknowledgements

This research was funded through grants from the Ministerio de Economía y Competitividad of Spain with the research project BIA2015-64672-C4-4-R. The experimental program was developed in the Laboratory of Concrete of the Institute of Concrete Science and Technology (ICITECH) of the Universitat Politècnica de València (UPV). Andrea Monserrat has been particularly supported by the Conselleria d'Educació, Investigació, Cultura i Esport of Generalitat Valenciana (Orden 6/2015, DOCV n. 7615 15.09.2015) with the European Regional Development Fund (ERDF) allocated by the EU.

VIC2D software was employed during the research stay of Andrea Monserrat at the EPFL (Lausanne, Switzerland).

References

ACI Committee 318. (2019). Building code requirements for structural concrete (ACI 318-19); and commentary (ACI 318R-19). American Concrete Institute.

Campana, S. *et al.* (2013). Analysis of shear-transfer actions on one-way RC members based on measured cracking pattern and failure kinematics. Magazine Concrete Research, 386-404.

Cavagnis, F., Fenández Ruiz, M., and Muttoni, A. (2018a). An analysis of the shear-transfer actions in reinforced concrete members without transverse reinforcement based on refined experimental measurements. Structural Concrete, 19 (1), 49-64.

Cavagnis, F., Fenández Ruiz, M., and Muttoni, A. (2018b). A mechanical model for failures in shear of members without transverse reinforcement based on development of a critical shear crack. Engineering Structures, 157, 300-315.

Cavagnis, F. *et al.* (2020). Shear strength of members without transverse reinforcement based on development of critical shear crack. ACI Structual Journal, 117, 103-118.

Correlated Solutions. (2009). VIC-2D Reference Manual.

EN 1992-1-1-2004. Eurocode 2: Design of concrete structures – Part 1-1: General rules and rules for buildings.

fib Bulletin 66 (2012). Model code 2010. Fédération Internationale du Béton (fib), Lausanne, Switzerland.

Guidotti, R. (2010). Poinçonnement des planchers-dalles avec colonnes superposées fortement sollicitées. EPFL, Lausanne (Switzerland).

Huber, P., Huber, T., and Kollegger, J. (2016). Investigation of the shear behavior of RC beams on the basis of measured crack kinematics. Engineering Structures, 113, 41-58.

Marí, A. *et al.* (2015). Shear-flexural strength mechanical model for the design and assessment of reinforced concrete beams. Structure and Infrastructure Engineering, 11 (11), 778-789

Marí, A. *et al.* (2016). Shear design and assessment of reinforced and prestressed concrete beams based on a mechanical model. Journal of Structural Engineering, 142 (10).

Monserrat López, A. *et al.* (2020a). Influence of the plastic hinge rotations on shear strength in continuous reinforced concrete beams with shear reinforcement. Engineering Structures, 207, 110242.

Monserrat López, A. *et al.* (2020b). Experimental study of shear strength in continuous reinforced concrete beams with and without shear reinforcement. Engineering Structures 220, 110967.

Huber, P., Huber, T., and Kollegger, J. (2016). Investigation of the shear behavior of RC beams on the basis of measured crack kinematics. Engineering Structures, 113, 41-58.

Muttoni, A., Fernández Ruiz, M. (2008). Shear strength of members without transverse reinforcement as function of critical shear crack width. ACI Structural Journal, 105 (2), 163-172.

Muttoni, A., Schwartz, J., and Thürlimann, B. (1997). Design of Concrete Structures with Stress Fields. Birkhaüser / Springer.

Reinhardt, H.W. (1985). Plain concrete modeled as an elastic strain-softening material at fracture. Engineering Fracture Mechanics. 22 (5), 787-796.

Schlaich, J., Schäfer, K. (1991). Design and detailing of structural concrete using strut-and-tie models. Structures Engineering, 69 (6), 113-125.

Schlaich, J., Schäfer, K., and Jennewein, M. (1987). Toward a consistent design of structural concrete. PCI Journal, 32, 74-150.

Sigrist, V. (1995). Zum Verformungsvermögen von Stahlbetonträgern (Deformation capacity of reinforced concrete beams). ETH, Zürich (Switzerland).

Vecchio, F.J., Collins, M.P. (1986). The Modified Compression-Field Theory for reinforced concrete elements subjected to shear. J. Proc., 83 (2), 219-231.

Walraven, J.C. (1981). Fundamental analysis of aggregate interlock. ASCE Journal Structural Division. 107 (11), 2245-2270.